Journal of Applied Polymer Science

The Cole–Cole plot for cure: The cure and reversion of natural rubber

Bryan G. Willoughby
Polymatrix, 84 White Hart, Reabrook Shrewsbury SY3 7TE, UK
Correspondence to: B. G. Willoughby (E-mail: bryan@polymatrix.co.uk)

ABSTRACT: Cure rheometry is routinely used in the rubber industry for processability assessment and cure-time determination. This article examines these rheological outputs in Cole–Cole format to explore what new insights can be gained from this alternative data plot. It differs from the conventional Cole–Cole treatment in its application to a reacting system. The plots described here are therefore of $G''(t)$ vs. $G'(t)$. Initially some attention is directed to the basics of the Cole–Cole treatment and the likely features to be expected when applied to systems undergoing both cure and reversion. This article goes on to consider examples of both by studying a natural rubber vulcanization at temperatures of 160 °C and above. Through the Cole–Cole approach, it is thought possible to identify the competition between intermolecular and intramolecular sulfurization, and between crosslink and main-chain scission. The approach offers considerable potential to expand the capabilities of cure rheometry. © 2016 Wiley Periodicals, Inc. J. Appl. Polym. Sci. **2016**, *133*, 44085.

KEYWORDS: crosslinking; degradation; rheology; rubber; viscosity and viscoelasticity

Received 23 March 2016; accepted 9 June 2016
DOI: 10.1002/app.44085

INTRODUCTION

The Cole–Cole plot is a form of Argand diagram, where the resolved components of a complex dynamic response are plotted against one another.[1] Thus, if the conventional format of a dynamic mechanical spectrum is a plot of $G'(\omega)$ and $G''(\omega)$ against the angular frequency ω, (where G' is the storage modulus, G'' the loss modulus, and ω the angular frequency), the Cole–Cole representation is a plot of $G''(\omega)$ against $G'(\omega)$.

Such plots have qualitative value in that the resultant shapes can be quite distinctive. For example, the plot appears to be specific to the molecular architecture, so that polymers having different types of branching (stars, combs, etc.), or markedly different MW distributions, generate distinctly different profiles. Given a suitable portfolio of reference traces, the Cole–Cole plot emerges as a novel and useful "fingerprinting" technique.

In principle, the same approach could be applied when a cure is monitored by oscillating rheometry. Thus when $G'(t)$ and $G''(t)$ are obtained against advancing cure time, a plot of $G''(t)$ vs. $G'(t)$ should remove the influence of time from time-dependent data. Conceptually, such a plot reflects the *route* rather than the *rate* of cure. By analogy with the application to dynamic mechanical spectroscopy, a plot of $G''(t)$ vs. $G'(t)$ may be able to shed light on the changing molecular architecture in the development of cure.

This possibility has relevance to the vulcanization of rubber, where oscillating rheometry is routinely used in cure monitoring.[2,3] A wealth of cure data is potentially available, either as the components of shear modulus or of complex torque [$S'(t)$ and $S''(t)$ vs. t]. To date, such cure rheometry has largely been used for processability assessment and cure-time determination. Is there more that can be learned from cure rheometry by applying the Cole–Cole approach?

One challenge, in vulcanization, is achieving the intended cure whilst avoiding heat ageing. Given the need to avoid premature cure in energy-intensive (i.e., heat-generating) mixing, the curing stage is likely to be designed to require temperatures of at least 140 °C. For useful productivity, with general purpose rubbers, temperatures of between 150 °C and 180 °C are more typical. But natural rubber (NR) is particularly sensitive to heat ageing, with a practical upper temperature limit for vulcanization of around 155 °C.[3] At higher temperatures, instability within the product network can result in cure reversal ("reversion").

One application of the Cole–Cole approach has been in the detection of chain scission and branching in the mechanical recycling of a thermoplastic.[4] This invites speculation on whether similar insights can be obtained from the Cole–Cole plot of an NR vulcanization—i.e., to distinguish the reactions of network formation and network scission. While the potential complexities of this approach should not be underestimated, the ready access to a wealth of data invites this exploration. Furthermore, there may be a special benefit here in that the $G''(t)$ vs. $G'(t)$ plot offers the potential to explore the balance between crosslinking and scission in real time. If this is shown to be the

Table I. Rubber Formulation

	phr
SMR L natural rubber	100.0
N990 MT carbon black	60.0
Strukdex 795 extender oil	7.0
Zinc oxide	5.0
Stearic acid	2.0
Cyclohexyl-2-benzothiazole sulfenamide	0.6
Sulfur	2.5
Octylated diphenylamine	1.0

case, then insights previously only accessible through time-consuming laboratory analysis, on research formulations, could be accessible on everyday products.

On this basis, the Cole–Cole plot could considerably expand the capabilities of cure rheometry. This article explores this potential. Working with a fully formulated rubber mix, it generates Cole–Cole plots for vulcanization and reversion, to seek to identify those diagnostic features which provide insights into the structural changes occurring.

EXPERIMENTAL

A sulfur-rich formulation (i.e., "conventional") was selected for study. It was chosen, from the mixes being processed at the time, as one representative of industrial practice in that it contained: filler, process oil, and a typical level of (hindered amine) stabilizer. The formulation used is listed in Table I.

Two-stage mixing was performed, the rubber, carbon black, extender oil, stearic acid, and zinc oxide being mixed in an internal mixer. The curatives, cyclohexyl-2-benzothiazole sulfenamide and sulfur were then added on a two-roll mill. The mix was then milled to a sheet and left to stand overnight before curing.

Samples for cure were placed in the preheated sample chamber (ca. 4.5 cm^3) of a Rubber Process Analyzer (RPA 2000, Alpha Technologies). The RPA 2000 is an oscillating rheometer with a pressurized-biconical die sharing the same geometry as the Moving Die Rheometer (MDR).[2] In these instruments, a sinusoidal strain is applied to the lower die and the toque response measured at the upper die. The phase difference between the two is also monitored. In these studies, the unvulcanized mix was introduced into the preheated die and the cures were monitored isothermally at 1.67 Hz and ±0.5° arc strain.

RESULTS AND DISCUSSION

The Cole–Cole Plot for Cure

Application to a reacting system marks a departure from the norm for the Cole–Cole treatment, and some thought should be given to the likely form of the resultant plot. A cure sees the balance between viscous and elastic character change over time, and some insight into the likely effect on $G'(t)$ and $G''(t)$ can be seen by reference to a simple mechanical model. One such model, which anticipates elastic character growing with increasing frequency, is the Maxwell model (Figure 1) which comprises a spring and dashpot in series.

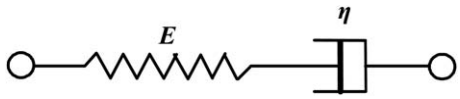

Figure 1. The Maxwell model of a spring and dashpot in series.

The dynamic response of this assembly can be analyzed in terms of an elastic modulus E for the spring, and a coefficient of viscosity η for the dashpot). The ratio of the two gives the time constant τ for stress relaxation ($\tau = \eta/E$). This assembly has a dynamic modulus (E^*) which is frequency dependent, as are its resolved components. The relationship with frequency is given by the following equations[5]:

$$E'(\omega) = E\tau^2\omega^2/(\tau^2\omega^2+1) \quad (1)$$

$$E''(\omega) = E\tau\omega/(\tau^2\omega^2+1) \quad (2)$$

where E' is the dynamic storage modulus and E'' the dynamic loss modulus.

From these expressions, it is possible to plot the frequency dependence of E' and E'' in dimensionless terms, i.e., as: E'/E and E''/E against a dimensionless frequency $\omega\tau$, as shown in Figure 2.

This plot of resolved components of modulus against frequency shows similarities to the cure profiles obtained by oscillating rheometry, notably those starting from a relatively low viscosity mix, where initially G'' and G' are very low, and G'' starts to rise before G'.[6] As plots of $G'(t)$ and $G''(t)$ against t, the cure profiles for the resolved components differ in that:

i. $G'(t)$ increases monotonically with time, reaching a maximum at the end of cure
ii. $G''(t)$ rises early in the cure and falls in the later stages.

In the Cole–Cole format, the data from Figure 2 take on a semicircular profile (Figure 3).

The level of correlation with real cures can be seen when Figure 3 is compared with plots derived from published data for two different liquid polymer cures. Figure 4 shows the $G''(t)$ vs. $G'(t)$ plots for: a 40 °C cast polyurethane cure and a room-temperature (RTV) liquid silicone cure.[6,7] Both were recorded

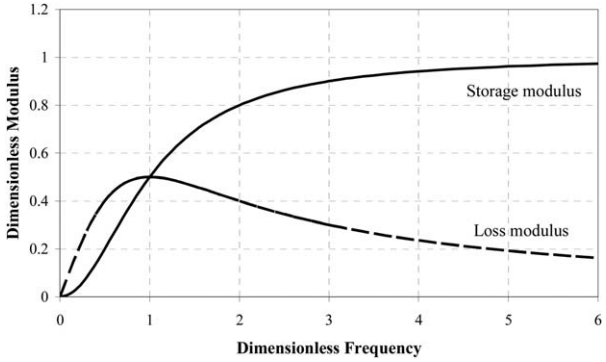

Figure 2. Plots of E'/E and E''/E against $\omega\tau$.

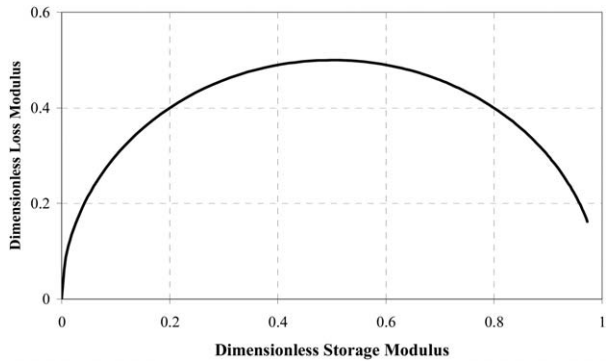

Figure 3. Cole–Cole plot from Figure 1.

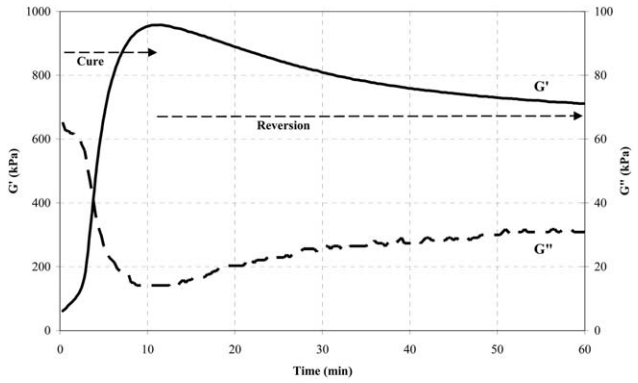

Figure 5. RPA traces for 160 °C cure of mix in Table I.

at fixed frequency on a cone-and-plate rheometer (1 Hz for PU, 0.16 Hz for silicone).

Although not semicircular, the Cole–Cole plots for these two real cures both show a distinct rise and fall with advancing cure. The two traces are similar in shape, but occupy different regions, with the PU reaching higher values of both G'' and G'.

The mid-cure maximum (in G'') in the Cole–Cole plot reflects the peak in the $G''(t)$ vs. t plots. This peak is commonly seen in cures of liquid systems, often in the vicinity of the gel time.[8,9] Nevertheless an exact correlation has not been demonstrated. In the case of the PU, gelation (at $G'' = G'$) occurs around 7.5 min, whereas G''_{max} occurs later at 11 min. Since G'' is a viscous (or friction) term, the pre-gelation rise can be linked with MW growth (chain extension). The later fall in G'' is somehow associated with the maturing network (crosslinking). Quite possibly, G''_{max} reflects some transition between the two.

By contrast, G' rises continuously with advancing cure and G' is taken to be proportional to crosslink density.[2,3] Since G'' is a friction term, then, at its simplest level, the Cole–Cole plot for cure might be taken as a plot of internal friction against crosslink density.

Rubber Vulcanization

As set out in the Introduction, the vulcanization of rubber will provide the starting point for more systematic analysis of the Cole–Cole plot for cure. Sulfur is the most commonly employed curative for diene rubbers, as it usually offers the best compromise in cure speed with adequate processing safety. Important variables in the cure include the level of sulfur (the curative) and the levels of coagents which influence its action. The coagents for the formulation in Table I are: the sulfenamide (CBS) accelerator and the ZnO/fatty acid activation system. A similar combination of 0.6 phr CBS and 5.0 phr ZnO with 2.5 phr sulfur in the vulcanization of a gumstock NR was studied in some detail by Porter, Skinner and Whelans, and found to achieve an optimum cure in about 40 min at 140 °C.[10] They found that a 20° increase had a major effect. At 160 °C, the optimum cure was reached in around 10 min. However, 50 min later, the crosslink density had fallen by nearly 50%.

For this present study, the mix was vulcanized in the preheated (and pressurized) sample chamber of the oscillating rheometer. This instrument (RPA 2000) provides complementary outputs of elastic and viscous torque (S' and S'') against time, and, within the linear-viscoelastic range (i.e., at very low strains), of storage and loss modulus (G' and G'') against time.[11] The complementary outputs of $G'(t)$ vs. t and $G''(t)$ vs. t for fixed-frequency monitoring of the 160 °C cure of this mix are shown in Figure 5.

Figure 5 is the format familiar to rubber technologists, and shows G' rising strongly in the first few minutes of cure and reaching a maximum after about 11 min. Reversion is expected for NR at this temperature and, once past this maximum, G' begins to fall. On the other hand, G'' seems to move in the opposite sense—i.e., falling as G' rises and rising as G' falls. In routine cure monitoring, only the storage component is used. Hitherto, there has been some uncertainty over the diagnostic value of the loss trace.[12]

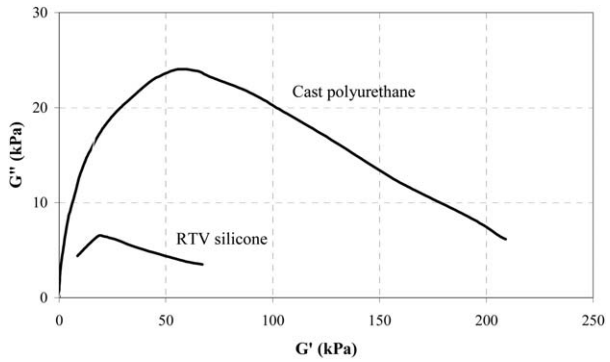

Figure 4. Plots of $G''(t)$ vs. $G'(t)$ for liquid elastomer cures.

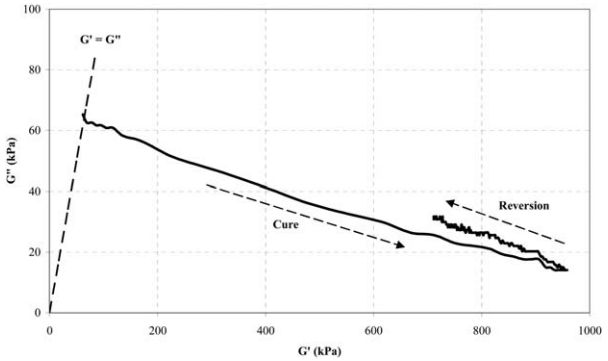

Figure 6. $G''(t)$ vs. G' (t) plot from Figure 5.

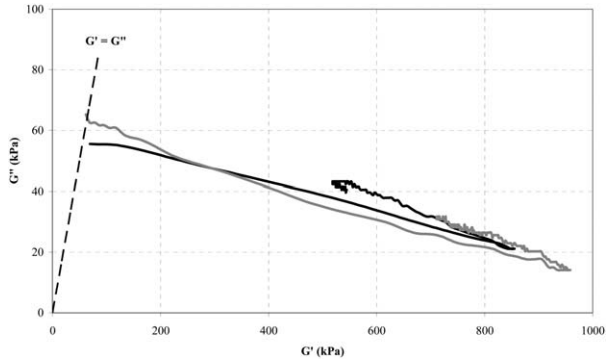

Figure 7. $G''(t)$ vs. $G'(t)$ plot for 180°C cure of mix in Table I.

On the other hand, there is widespread acceptance that the $G'(t)$ vs. t trace reflects the changing crosslink density. Since rubber cure rheometry is characteristically conducted at elevated temperature, the network changes being monitored are most likely to involve the primary linkages. Thus the $G'(t)$ vs. t plot has become the established tool for monitoring the progress of chemical crosslinking in rubber. The uncertainty regarding the diagnostic value of $G''(t)$ vs. t trace means that this is usually ignored.

Figure 6 shows the data from Figure 5 reproduced in the Cole–Cole format. It also shows the $G'' = G'$ gel line—i.e., the line nominally separating liquid from solid. To the left of the line ($G'' > G'$), the sample is an elastoviscous liquid and to the right of the line ($G' > G''$), the sample is a viscolelastic solid. The trace sits almost completely to the right of this line, reflecting the case that this rubber is substantially gelled from the outset.

From the start, the cure trace falls in the manner of the later stages of the two liquid elastomer cures in Figure 4.

Since G' rises with crosslink density, the transition from cure to reversion shows up especially clearly as a Cole–Cole plot. There is a marked discontinuity at the onset of reversion, where the trace turns back on itself. G' falls with reversion and G'' rises. Superficially it appears that the reversion here is simply a reversal of the cure, with the cure path almost retracing its original route.

The change in direction has particular significance. If the reversion is an exact reversal of the route of cure, then the reversion must reverse the reactions of cure—i.e., must involve crosslink scission.

Effect of Temperature

The above statement applies if the reactions of cure are purely crosslinking. Such apparent simplicity will be lost if there are noncrosslinking side reactions running alongside the cure. This is indeed the case for the sulfur vulcanization of diene polymers, where backbone changes result. Morrison and Porter saw the sulfur vulcanization of NR as a temperature-dependent balance of reactions leading either to crosslinks or to backbone modifications.[13] They considered the weakest link in the network as the polysulfidic S−S bond, and described the formation of cyclic sulfides and disulfides, together with conjugated dienes and trienes, from the thermal breakdown of polysulfidic crosslinks. Zinc sulfide is also formed and these various changes, which can be effective from temperatures as low as 140 °C, were summarized according to the following equation:

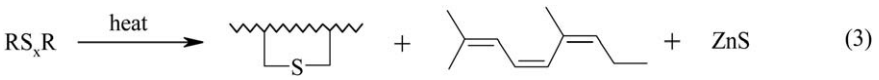

Similar conclusions have been drawn from curve-fitting to RPA cure profiles, where a parameter ψ was used to cover the competition between crosslinking and nonproductive side reactions.[14] This modelling anticipated an exponential dependency on temperature for ψ, such that balance shifts increasingly away from crosslinking as temperature rises.

The effect of increasing temperature on the $G''(t)$ vs. $G'(t)$ plots for this mix can be seen in Figures 7 and 8. Figure 7 shows the $G''(t)$ vs. $G'(t)$ plot for the mix at 180 °C (with the 160 °C cure shown in grey). Figure 8 shows the $G''(t)$ vs. $G'(t)$ plot for the 60 min/200 °C cure (with the 180 °C cure shown in grey).

With respect to Figure 7, the two cures appear to be following roughly similar courses, although there are detailed differences. The start in terms of G' is slightly higher for the higher temperature cure, which suggests this cure to be a little more advanced at the first recording point. In terms of G'', the starting point is lower for the higher temperature cure as might be expected for the effect of temperature on the viscosity of a polymer melt. The two traces cross-mid-cure, implying that their slopes are different.

As might be anticipated from the competition from noncrosslinking side reactions, the point of maximum cure, G'_{max}, is lower at 180 °C cure than for 160 °C. This reflects the effect of temperature seen in the model compound studies of Porter, Skinner, and Whelans.[10]

The difference between the values of G'_{max} is also reflected in a higher level of reversion for the higher temperature cure—again

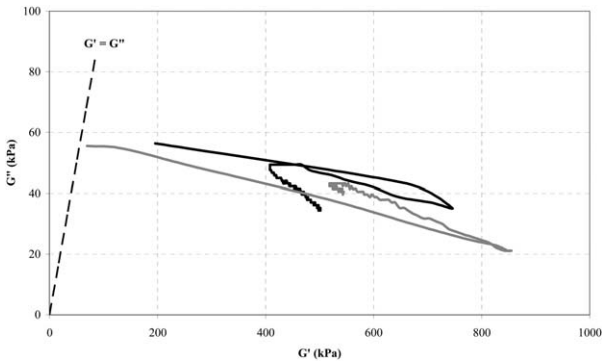

Figure 8. $G''(t)$ vs. $G'(t)$ plot for 200°C cure of mix in Table I.

Table II. Coordinates for M_L and M_H on $G''(t)$ vs. $G'(t)$ plots (Figures 6–8)

	M_L		M_H		
Temp (°C)	G'' (kPa)	G' (kPa)	G'' (kPa)	G' (kPa)	Slope $M_L \rightarrow M_H$
160	65.2	61.7	14.1	958	−0.057
180	55.5	69.6	21.1	855	−0.044
200	56.4	197	36.0	745	−0.037

reflecting the trends in the model compound study. Over 60 min, G' for the 160 °C cure has fallen back to 710 kPa, whereas the same time for the 180 °C cure sees G' fall nearly 200 kPa. Interestingly the minimum (~520 kPa) is reached after 30 min' cure and, from then on, G' starts to rise again—suggesting, perhaps, a *reversal* in the reversion.

At 200 °C, the start in terms of G' is even higher that at 180 °C, which points to a cure which is even more advanced at the start of monitoring. Figure 8 shows that the starting point is now well away from the $G'' = G'$ gel line and, interestingly, G'' also starts higher than at 180 °C. The uplift for G'' cannot be accounted for as a temperature–viscosity effect and points to some other influence at work. In some way, an increase in internal friction is resulting from the onset of the 200 °C cure.

With respect to G'_{max}, it can be seen that the trend in Figure 7 is continued in Figure 8—i.e., G'_{max} continues to fall as the cure temperature increases. The decreasing values of G'_{max} with increasing temperature are shown in Table II. As with Figure 7, the outward (cure) traces in Figure 8 appear to be diverging. This looks to continue the trend of Figure 7, so that, over the 160–200 °C range, the downward slope (of cure) appears to be reducing with rising temperature.

That there is a consistent trend between slope and temperature can be determined from the respective coordinates (as G'' and G') for the start- and end-points of the curing stage. These correspond to the lowest and highest values of G', which, in rubber technology, are commonly designated M_L (for G'_{min}) and M_H (for G'_{max}). Table II lists these coordinates and the mean gradients for all three temperatures. The change, although relatively small, shows that the plots for the curing stage are falling less steeply as the temperature rises—i.e., the gradient is rising with increasing temperature.

The shifts in G'' at M_L have already been mentioned, and may reflect competition between a physical effect (temperature) and a chemical effect (cure). The trend in gradients suggests that, as cure advances, internal friction is changing at different rates at different temperatures. Thus, a higher temperature cure sees a progressive increase in internal friction, and this shift is evident even at the start of the 200 °C cure.

Internal friction is expected to bear some relationship with T_g. Possible evidence for this is seen in Figure 4 where the higher values of G'' for the polyurethane cure reflect the higher value of T_g for the starting polymer. For the two starting polymers here, the respective values are: −62 °C for polypropylene oxide (for the polyether-urethane) and −123 °C for polydimethylsiloxane.[15] However, Figure 4 does not provide an ideal basis for comparison as the monitoring frequencies for the two cures are different. The operating temperatures are slightly different also.

A better comparison is seen in the cure rheometry of Dick, Pawlowski and Scheers.[12] These studies embraced a host of different rubber polymers and found that, under standard conditions (same oscillating frequency, strain amplitude, and temperature), the peak in viscous torque came later in the cure for less resilient (higher T_g) elastomers. Separate work by this present author can confirm this trend, and can also add that a later peak equates to a larger peak. Additionally, Dick, Pawlowski, and Scheers found that viscous torque rose with increasing loadings of carbon black (reinforcement) and fell with the addition of process oil (plasticization). These various findings support the idea of a relationship between the loss response and T_g, where G'' or S'' rises with increasing T_g. In which case, one possible implication, from the changing slopes in Table II, is that T_g is changing during the cure and at different rates at different temperatures. The anticipated effect on slope is presented schematically in Figure 9.

By this interpretation, the rising slope with increasing temperature equates to an increasing T_g (stiffening of the backbone). This is consistent with the expectations from eq. (3). Any cyclization can be expected to stiffen the backbone. In the case of the acid-catalyzed cyclization of NR, the T_g can rise to above room temperature.[16] The stiffening effect of conjugated triene sequences can be seen in the extreme case of polyacetylene, where the T_g rises to above 150 °C.[17] Thus a self-consistent picture emerges where both the slope of the $G''(t)$ vs. $G'(t)$ plot and the value of G'_{max} reflect the differing contributions of crosslinking and nonproductive side reactions.

Attention just to the slopes of these plots implies that the changing balance of reactions can be seen even *before* the onset of reversion. This suggests that the susceptibility to reversion can be anticipated for even those cases where monitoring was stopped at M_H. In principle, the same would be possible from the curve-fitting work of Ding, Leonov, and Coran.[14] However their parameter ψ (for the competition between crosslinking

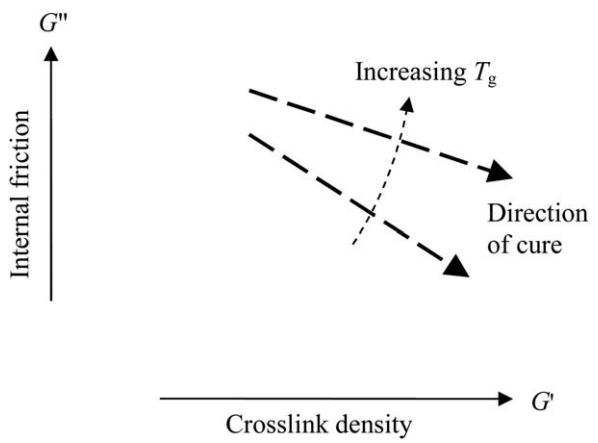

Figure 9. Possible effect of changing T_g on the $G''(t)$ vs. $G'(t)$ plot for NR cure.

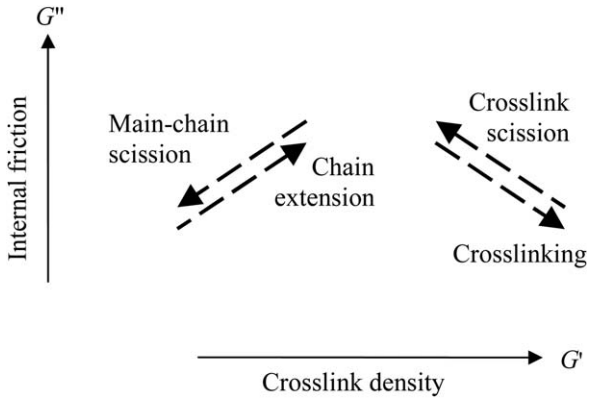

Figure 10. Possible significance of rising and falling slopes in the $G''(t)$ vs. $G'(t)$ plot.

and nonproductive side reactions) was one of four different parameters used in the curve-fitting process. The inherent complexity may reflect the attempt to model the effect of competing rate effects on a single output of the RPA—namely a plot of $G'(t)$ vs. t. By using both outputs, such that the effect of time is removed, different cures may be overlaid so that subtle differences are easier to detect. Thus, as seen with nonreacting systems, the Cole–Cole plot for cure holds promise of a novel and useful "fingerprinting" technique. With familiarity, the Cole–Cole plot of cure could become a powerful tool in compound development.

Reversion

If plotting the route, rather than the rate, of cure allows subtle differences to be more readily seen, the plot provides an especially clear indication if major changes occur. With the onset of reversion, the process of crosslinking is reversed, and G' passes through a sharply defined maximum. Visually, the $G''(t)$ vs. $G'(t)$ plot turns back on itself. As mentioned earlier, if the reversion is an exact reversal of the route of cure, then this must reverse the reactions of cure—i.e., the reversion involves crosslink scission.

This is a point that can be amplified by reference to Figure 4, which shows the $G''(t)$ vs. $G'(t)$ plot from relatively low MW

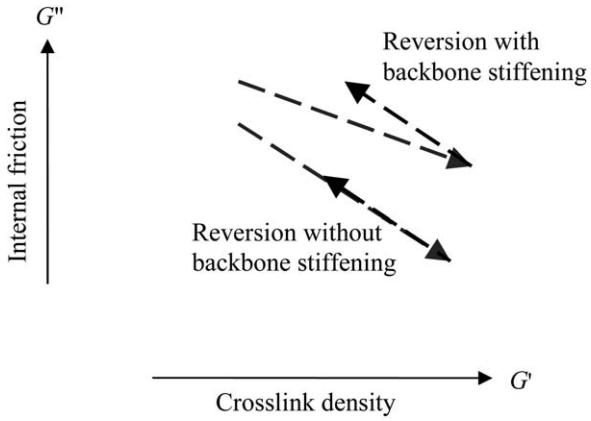

Figure 11. Anticipated divergence in cure and reversion routes arising from because of backbone stiffening.

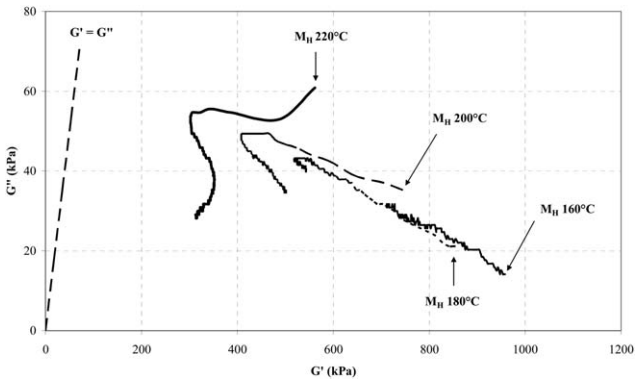

Figure 12. $G''(t)$ vs. $G'(t)$ plots for reversion stages of 160–220°C cures.

starting materials. If the early rise in G'' is largely associated with chain extension, and the later fall in G'' is linked to crosslinking, then the rising and falling slopes of the $G''(t)$ vs. $G'(t)$ plot must have similar connotations. It follows from this that if the slopes are reversed, then the reverse process is occurring. By this argument, the significance of the respective reversals is as shown in Figure 10.

While Figure 10 may indicate the significance of rising and falling slopes in the respective cure or reversion traces, the actual values of the gradients will still be hostage to the balance of reactions occurring. Thus a side reaction which progressively increases G'' during cure will have the same effect if it continues into reversion. As a result, the outward (cure) and return (reversion) will diverge as indicated in Figure 11.

On this basis, a divergence as suggested in Figure 11 can also be taken as further evidence for backbone stiffening. Both the 160 °C and 180 °C cures show some divergence (Figures 6 and 7). Thus, as might be expected from the supporting chemistry, even the 160 °C cure is not free of such side reactions.

However, the same is not seen for the 200 °C study, even though the outward route sits markedly higher than that at the lower temperatures. Here the continued progression to higher G'' does not extend to the reversion. Now the initial reversion appears to be on a lower course. This suggests there are further changes occurring, with some stiffer elements being removed. Morrison and Porter reported that open-chain structures containing —CH=S or —SH attachments are formed at temperatures above 180 °C.[13] It could be that these are formed by breakdown of cyclic sulfides.

To explore further the effect of temperature, the study was extended to 220 °C. This is a catastrophically high temperature for cure with NR, and the rheometer trace seems to be wholly that of reversion (i.e., M_L is also M_H). In line with the other cures of this study, this monitoring was performed over the full 60 min, and the Cole–Cole plot is shown in Figure 12, alongside the reversion stages for the other three temperatures.

The absence of a defined cure trace at 220 °C means that it is not possible to establish whether the reversion sets out on a lower course (with respect to G''). However, it is interesting to note that, initially at least, this 220 °C trace is heading towards the course (or projected course) of the three lower temperature reversions. The

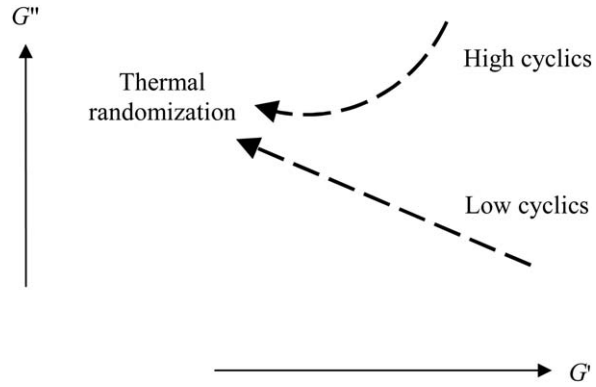

Figure 13. Possible effect of thermal randomization in NR reversion.

impression gained is that, for the early stages, these reversions are heading towards a common product. Various stiffening elements (crosslinks, backbone cyclizations, etc.) are being removed in processes which can be regarded as entropy driven.

Entropy is a recognized driver in a further side reaction of NR in vulcanization (and reversion). This is *cis-trans* isomerism, in which the stereoregular polyisoprene is converted, over time, into an equilibrium mix of isomers.[18,19] The longer the time at temperature, the more extensive the randomization. Collectively all these backbone changes can be viewed as a thermal randomization. If allowed to follow its natural course, a common structure would result. Schematically this might be represented by Figure 13.

Reversal of Reversion

The reality of Figure 12 is that this thermal randomization is not allowed to follow its natural course, as there is another change which takes over. Three of the traces show regions where the reversion apparently goes into reverse—i.e., where G' starts to rise again. This rise in G' corresponds to a fall in G'', a combination suggesting crosslinking. (e.g., Figure 10).

It seems unlikely that any fresh crosslinking will be sulfidic, as it is the instability of these linkages which is thought to start the reversion. This invites speculation of how other crosslinking becomes feasible. One possible source of new crosslinking is the enhanced reactivity from the conjugated triene structures in eq. (3). Conjugated trienes are detectable by IR spectroscopy and first appear at the onset of reversion.[20] The growth in conjugated triene has been monitored in NR cures for up to 60 min at 150 °C. As yet, no data have been located for concentrations at higher temperatures, or for longer times, but it seems unlikely that such a reactive structure would survive for long in a hot rubber mix. For example, the conjugated-triene structure can be considered a fragment of polyacetylene—a polymer susceptible to oxidative crosslinking.[21]

Particular reactivity arises from the introduction of the more accessible —CH=CH— double bond. Polybutadiene is readily crosslinked by peroxides; with high crosslinking efficiencies indicative of chain reactions.[22] This invites speculation on the carbon-centered radicals present in the heat ageing of a sulfur vulcanizate of NR.

The weak link in the in 1,4-polyisoprene chain, at ~230 kJ/mole, is the C−C bond joining successive isoprene units (Figure 14).[23] This is well down on typical C−C bond strengths, and at a level more commonly associated with S−S bonds. The bonds in sulfur chains are weaker than in rings, and the thermal cleavage of polysulfides is considered the starting point for reversion.[13,24] Nevertheless, it may be that C−C scission is not far behind.

If the implication here is that the polysulfidic thiyl radical, $S_xS\bullet$, is (marginally) more stable than the allylic carbon radical, then the sequence of bond stabilities would be:

$$_{(\text{polysulfidic})}\text{S}-\text{S}_{(\text{polysulfidic})} \leq {}_{(\text{polysulfidic})}\text{S}-\text{C}_{(\text{allylic})} \leq {}_{(\text{allylic})}\text{C}-\text{C}_{(\text{allylic})}.$$

On this basis crosslink scission precedes backbone scission—but only just. Backbone scission creates allylic carbon radicals which have the potential to initiate a chain polymerization of the triene sequences. However, given that conjugated-triene sequences may be sparsely distributed along the backbone, the initiating radicals may reach an excess relatively quickly, and the predominant reaction may be simply that of initiator addition ($\text{I}\bullet + \text{M} + \bullet\text{I} \rightarrow \text{IMI}$). This could take the form of eq. (4), whereby two chains are joined together in the manner of a single crosslink. Since the addition site (−CH = CH−) arises from elimination of a sulfur crosslink, eq. (4) effectively replaces a former crosslink. This puts the reversion into reverse, and the cure appears to start again:

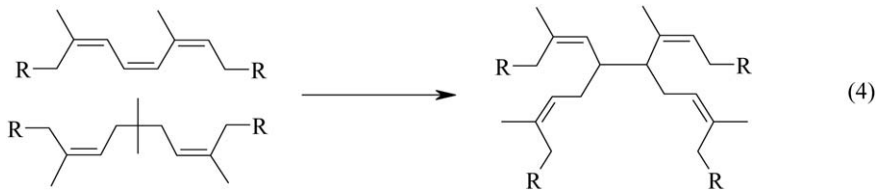

(4)

By this hypothesis, this second-stage crosslinking ends when the conjugated triene is used up. From this point onwards, the continued backbone scission will progressively break up the network, and the fragments released will act as plasticizers. In a vulcanizate, plasticization reduces both G' and G''.[12] In which case, increasing levels of backbone scission will see the $G''(t)$ vs. $G'(t)$ plot falling downwards and to the left, as was anticipated in Figure 10.

A sequence where crosslinking is initiated and then is overcome by backbone scission can explain the later stages of 220 °C plot

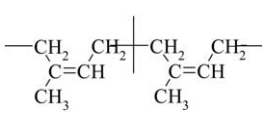

Figure 14. Weak link in the 1,4-polyisoprene chain.

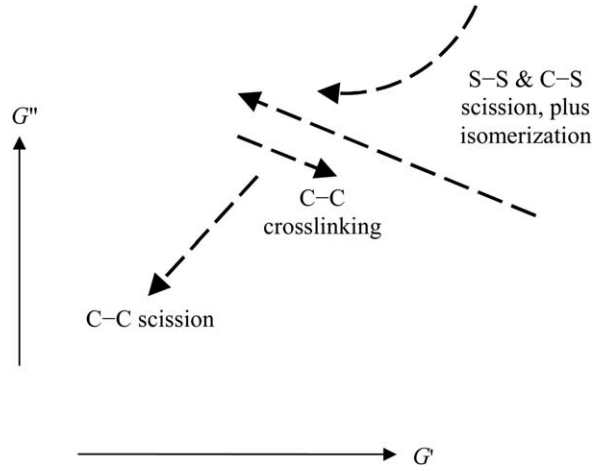

Figure 15. Possible influences on the $G''(t)$ vs. $G'(t)$ plot for NR reversion.

in Figure 12. Collectively, the twists and turns of the whole 220 °C plot can be interpreted in terms of sequential processes in reversion, starting at linkages to sulfur but eventually moving on to main-chain scission. The lower temperature plots see this followed to different degrees. Conceptually, the whole of Figure 10 can be interpreted in terms of different bond instabilities as is suggested in Figure 15.

While the picture presented in Figure 15 may offer no surprises, its derivation from cure rheometry is surely remarkable. As with cure, it is the ability to overlay traces in the Cole–Cole format which allows similarities and differences to be more easily recognized. In essence, like fingerprinting, it is a visual comparative technique.

There is perhaps one feature of Figure 12 which merits special mention. Even at 220 °C, the reversion sits well to the right of the $G'' = G'$ line—i.e., the material remains firmly in the solid phase. It is clearly apparent that the original route of cure is not being retraced. Reversion is not cure reversal, it is heat ageing, and the difference is unmistakable in the Cole–Cole format. For NR, heat is therefore a barrier to cure reversal. This is an aspect of reclaiming strategies which is often ignored. Perhaps a fresh perspective is needed. If so, the Cole–Cole plot may have a valuable role to play.

CONCLUSIONS

The Cole–Cole plot for cure [$G''(t)$ vs. $G'(t)$] takes time out of consideration so that the resultant trace reflects the route rather than rate of cure. It allows cures of different rates to be overlaid so that similarities or differences may be more easily seen. Conceptually, it is a plot of internal friction against crosslink density. Internal friction rises with increasing chain length, but falls as crosslinking takes over. It also rises with increasing chain stiffness—i.e., with T_g.

G' provides a measure of crosslink density, and thus the slope of the $G''(t)$ vs. $G'(t)$ reflects the changes in internal friction as crosslinking advances. Side reactions which stiffen the backbone (e.g., cyclization) raise the slope. If these reactions also compete with crosslinking, then the attainable crosslink density, measured by G'_{max}, will fall. This effect is seen in these NR cures.

Now it must follow that, if the creation of crosslinks sees G'' fall as G' rises, then their subsequent loss from the network should see G'' rise as G' falls. Thus a rise in G'' with falling G' can be taken as indicative of main-chain scission.

The same principle of reversibility should apply to the rise in G'' with increasing chain length. If G'' rises with increasing chain length, then G'' should fall with chain scission. Hence a fall in G'' with falling G' can be taken as indicative of crosslink scission.

On this basis, it should be possible to recognise backbone modifications (stiffening), and distinguish crosslink scission from main-chain scission. Thus, in the case of these NR cures, it is proposed that $G''(t)$ vs. $G'(t)$ plot from cure rheometry can reveal:

i. the balance between intermolecular and intramolecular sulfurization in cure
ii. the balance between crosslink scission and main-chain scission in reversion.

Importantly, the plot also provides evidence for some crosslinking in the later stages of reversion, which is attributed here to C − C crosslinking. These various backbone changes mean that the outward (cure) route cannot be retraced by thermal reversion—as is clearly seen on the $G''(t)$ vs. $G'(t)$ plot.

Indeed the differing courses of both cure and reversion are put in a visual context by $G''(t)$ vs. $G'(t)$ plot. As shown here, it can significantly expand the capabilities of cure rheometry.

ACKNOWLEDGMENTS

This research exercise was conducted when the author was a consultant to Rapra Technology Ltd (now Smithers Rapra) at their laboratories in Shawbury, UK. The provision of materials and equipment is gratefully acknowledged. The author is particularly indebted to John Manley for the supply of the rubber compound and to Mark Edwards for operation of the Rubber Process Analyzer.

REFERENCES

1. Dealy, J. M.; Larson, R. G. Structure and Rheology of Molten Polymers; Carl Hanser Verlag: Munich, **2006**; Chapter 5, p 176.
2. Dick, J. S. In Rubber Technology Compounding and Testing for Performance; Dick, J. S., Ed.; Carl Hanser Verlag: Munich, **2009**; Chapter 2, p 25.
3. Coran, A. Y. In The Science and Technology of Rubber, 3rd ed.; Mark, J. E., Erman, B., Eirich, F. R., Eds.; Elsevier: Amsterdam, **2005**; Chapter 7, p 324.
4. Nait-Ali, K. L.; Bergeret, L.; Ferry, L.; Colin, X. *Polym. Test.* **2012**, *31*, 500.
5. Ferry, J. D. Viscoelastic Properties of Polymers; Wiley: New York, **1961**; Chapter 3, p 42.
6. Willoughby, B. G. Physical and Chemical Methods of Cure Monitoring, presented at the POLMATIN Workshop

Standardisation, Measurement and Testing (SMT) of polymer Materials for Better Quality of Life; ICRI: Warsaw, October 9–10, **2003**.

7. Valles, E. M.; Macosko, C. W. *Macromolecules* **1979**, *12*, 673.
8. Malkin, A. Ya.; Kulichikhin,S. G. Rheokinetics; Huthig and Wepf: Heidelberg, **1996**; Chapter 3, p 142.
9. ASTM Standard D4473-03, Standard Test Method for Plastics: Dynamic Mechanical Properties, Cure Behavior; ASTM International, West Conshohoken, PA.
10. Porter, M.; Skinner, T. D.; Wheelans, M. A. *J. Appl. Polym. Sci.* **1967**, *11*, 2271.
11. Lee, S.; Pawlowski, H.; Coran, A. Y. *Rubber Chem. Technol.* **1994**, *67*, 854.
12. Dick, J. S.; Pawlowski, H.; Scheers, E. *Polym. Test.* **1995**, *14*, 45.
13. Morrison, N. J.; Porter, M. *Rubber Chem. Technol.* **1984**, *57*, 63.
14. Ding, R.; Leonov, A. I.; Coran, A. Y. *Rubber Chem. Technol.* **1996**, *69*, 81.
15. Armeniades, C. D.; Baer, E. In Introduction to Polymer Science and Technology; Kaufman, H. S., Falcetta, J. J., Eds.; Wiley-Interscience: New York, **1977**; Chapter 6, p 276.
16. Riyajan, S.; Sakdapipanich, J. T. *Kautsch. Gummi Kunstst* **2006**, *59*, 104.
17. Masuda, T.; Tang, B. -Z.; Tanaka, A.; Higashimura, T. *Macromolecules* **1986**, *19*, 1459.
18. Golub, M. A. In Chemical Reactions of Polymers, Fettes, E. M., Ed.; Interscience: New York, **1964**; Chapter IIA, p 121.
19. Koenig, J. L. *Rubber Chem. Technol.* **2000**, *73*, 385.
20. Chen, C. H.; Koenig, J. L.; Shelton, J. R.; Collins, E. A. *Rubber Chem. Technol.* **1981**, *54*, 734.
21. Will, F. G.; McKee, D. W. *J. Polym. Sci. A Polym. Chem.* **1983**, *21*, 3479.
22. Loan, L. D. *Rubber Chem. Technol.* **1967**, *40*, 149.
23. Golub, M. A. *Pure Appl. Chem.* **1972**, *30*, 105.
24. Meyer, B. *Chem. Rev.* **1976**, *76*, 367.